Pergamon

Polyhedron Vol. 17, No. 23–24, pp. 4203–4212, 1998
© 1998 Elsevier Science Ltd
All rights reserved. Printed in Great Britain
0277–5387/98 \$19.00+0.00

PII: S0277–5387(98)00230–7

X-ray crystal structures of $Mo_3S_4(DTP)_3(salicylate)(CH_3CN)$ and $[Mo_3S_4(DTP)_3(phthalate)(Py)]_2 \cdot EtOH \cdot CH_2Cl_2$: intramolecular H-bonds and S–S interactions in trinuclear molybdenum cluster compounds

Ling Wu, Jibo Xia, Changneng Chen, Xiaoying Huang, Yuangen Yao† and Jiaxi Lu

State Laboratory of Structural Chemistry, Fujian Institution of Research on the Structure of Matter,
Chinese Academy of Sciences, Box 143, Fuzhou, 350002, P.R. China

(Received 14 January 1998; accepted 8 June 1998)

Abstract—Two new molybdenum cluster compounds, $Mo_3S_4(DTP)_3(salicylate)(CH_3CN)$ and $[Mo_3S_4(DTP)_3(phthalate)(Py)]_2 \cdot EtOH \cdot CH_2Cl_2$, have been rationally synthesized by the ligand substitutional reaction of $Mo_3S_4(DTP)_4(H_2O)$ with salicylic acid and phthalic acid, respectively. Their crystal structures have been determined. A molecular-design method for Mo_3S_4 cluster compounds was developed. Two incomplete cuboidal molybdenum cluster units can be linked by intramolecular H-bonds. © 1998 Elsevier Science Ltd. All rights reserved

Keywords: synthesis; X-ray structure; H-bond; S–S interaction; aromatic carboxylate; NMR.

INTRODUCTION

Since the trinuclear molybdenum cluster compound $Mo_3S_4(\mu\text{-DTP})(DTP)_3(L)$, where L = loosely-coordinated ligand, DTP = diethyldithiophosphate, (**I**) was reported [1], several new clusters formulated as $Mo_3S_4(\mu\text{-RCO}_2)(DTP)_3(L)$ (**II**) were synthesized by substitution reactions [2]. It is now well established that this Mo_3S_4 precursor **I**, unlike its aqueous analogous cation $[Mo_3S_4(H_2O)_9]^{4+}$, has three different substitutional sites: bridging DTP, terminal DTP [3] and the loosely-coordinated ligand L. By choosing ligands of different chemical properties for the precursor **I**, we can now control the molecular fragmentation to design molybdenum cluster molecules suitable for potential applications, for example, in the exploitation of catalytic reactions promoted at a metal site embedded in metal–sulfur aggregates [4, 5]; in the synthesis of new optical limiting materials [6]. Aromatic carboxylic acids, which can bond with various functional groups, were considered in this paper as the substituting reagents for the bridging DTP ligand.

In our preliminary experiments, the reaction of **I** with benzoic acid yielded a brown powder which was difficult to dissolve in any solvent, making the crystal structure determination impossible. However, we isolated well-formed crystals of $Mo_3S_4(DTP)_3(salicylate)(CH_3CN)$ (**III**) and $[Mo_3S_4(DTP)_3(phthalate)(Py)]_2 \cdot EtOH \cdot CH_2Cl_2$ (**IV**) by the reaction with salicylic acid and phthalic acid, respectively. Compared with the earlier experimental results, this paper provides a further molecular-design method for Mo_3S_4 cluster compounds.

EXPERIMENTAL

General procedure

$Mo_3S_4(DTP)_4(H_2O)$ was obtained by the method of literature [3]. HDTP was purified before used by vacuum distillation [7]. Phthalic acid, salicylic acid, dichloromethane and pyridine are commercially avail-

---

† Author to whom correspondence should be addressed.

able A.R. grade reagents which are used without further purification. The whole experiments were handled free of water. IR spectra were recorded on Nicolet Magna 750 and FTS-40 spectrometers in KBr pellets. ^{31}P NMR spectra were measured on an Varian Unity-500 NMR spectrometer in deuterated acetone [3] with reference to 85% H_3PO_4. Spectra were first recorded in 100.0 kHz width and then enlarged to a suitable scale.

Preparation of $Mo_3S_4(DTP)_3(salicylate)(CH_3CN)$ (**III**): in a flask, 0.3 g $Mo_3S_4(DTP)_4(H_2O)$ was dissolved in 40 cm^3 of mixed solvent of ethanol and acetonitrile (v/v = 3:1). 0.03 g salicylic acid was then added while stirring. When refluxed over an oil bath at 100°C for an hour, the hot dark brown solution was filtered into another flask. Rectangular black crystals precipitated in 10 days. Yield: 0.18 g, 60%. Found: Mo, 25.18; C, 21.76; H, 3.31; N, 1.06; Calc. for $C_{21}H_{38}Mo_3NO_9P_3S_{10}$: Mo, 25.03; C, 21.94; H, 3.33; N, 1.22.

Preparation of $[Mo_3S_4(DTP)_3(phthalate)(Py)]_2 \cdot EtOH \cdot CH_2Cl_2$ (**IV**): 0.20 g of $Mo_3S_4(DTP)_4H_2O$ was dissolved in 30 cm^3 dichloromethane and 20 cm^3 ethanol. The solution was then refluxed over an oil bath at 100°C with 0.03 g phthalic acid and 0.2 cm^3 pyridine for an hour. When filtered and cooled to room temperature, this black solution gave well-shaped rectangular black crystals in two weeks. Yield 0.15 g (70%). Found: Mo, 22.30; C, 24.25; H, 3.21; N, 1.06; Calc. for $C_{53}H_{88}Cl_2Mo_6N_2O_{21}P_6S_{20}$: Mo, 22.46; C, 24.84; H, 3.46; N, 1.09.

X-ray structure determinations

The crystal data for compounds **III** and **IV** are summarized in Table 1. The important bond lengths and angles for the complex **III** and **IV** are given in Tables 2 and 3. Single crystals for **III** and **IV** were carefully chosen, coated with epoxy resin and mounted on glass fibers. Data collections and cell dimension measurements were performed on Siemens SMART CCD diffractometer with graphite-monochromatized Mo–Kα radiation ($\lambda = 0.71073$ Å) at 21 ± 2°C. Intensity data for all crystals were obtained in the range $3.08 < 2\theta < 46.6°$ by using an ω scan technique. The data reductions and structural analysis were performed on a silicon computer station with Smart CCD software and the structure were refined on F^2 through the use of the SHELXL-PC programs [8, 9, 10]. Empirical absorption corrections were applied. The positions of the molybdenum atoms were determined by direct methods, and successive difference electron density maps located the remaining nonhydrogen

Table 1. Crystallographic data and some experimental details for complexes **III** and **IV**

Compound	Complex **III**	Complex **IV**
Chemical formula	$C_{21}H_{38}Mo_3NO_9P_3S_{10}$	$C_{53}H_{88}Cl_2Mo_6N_2O_{21}P_6S_{20}$
Formula weight	1149.80	2562.87
Color	black	black
Crystal dimension (mm)	0.10 × 0.15 × 0.20	0.15 × 0.15 × 0.20
Crystal system	triclinic	triclinic
Space group	$P\bar{1}$	$P\bar{1}$
F (000)	1132	2560
a (Å)	13.506(3)	15.692(0)
b (Å)	13.546(3)	15.707(8)
c (Å)	15.026(3)	22.603(3)
α (°)	72.64(3)	99.395(1)
β (°)	65.96(3)	93.164(1)
γ (°)	60.67(3)	115.883(1)
V (Å^3)	2171.84(0)	4894.85(11)
Z	2	2
D_{calc} (g cm^{-3})	1.74(6)	1.73(6)
Temp (K)	296(2)	293(2)
μ (mm^{-1})	1.380	1.383
No. of refl. collected	8569	19117
No. of refl. observed	5102($>4\sigma$)	11272($>2\sigma$)
R	0.0530	0.0553
R_w	0.0713	0.1286
Goodness of fit. S	1.88	1.138
Parameters refined	400	903
Largest shift	0.025	0.024
Largest different peak (e Å^{-3})	0.91	1.29

$R = \Sigma \| F_0 | - | F_c \| / \Sigma | F_0 |$. $R_w = [\Sigma w(|F_0| - |F_c|)^2 / \Sigma w |F_0|^2]^{1/2}$.

Table 2. Selected bond length (Å) and angles (°) for the complex **III**

Mo(1)–Mo(2)	2.763(1)		
Mo(1)–Mo(3)	2.765(1)		
Mo(1)–S	2.339(2)		
Mo(1)–S(1)	2.302(3)		
Mo(1)–S(2)	2.282(2)		
Mo(1)–N	2.269(7)		
Mo(2)–Mo(3)	2.693(2)		
Mo(2)–S(3)	2.289(2)		
Mo(2)–S	2.350(3)		
Mo(2)–S(1)	2.294(2)		
Mo(2)–O(2)	2.244(6)		
Mo(3)–S(3)	2.290(3)		
Mo(3)–S	2.346(2)		
Mo(3)–S(2)	2.297(2)		
Mo(3)–O(1)	2.252(5)		
O(2)–C	1.29(2)		
O(1)–C	1.26(1)		
O(3)–H(3A)	0.850		
O(3)–C(2)	1.35(2)	Mo(1)–Mo(3)–S(3)	97.0(1)
Mo(2)–Mo(1)–Mo(3)	58.3(1)	S(3)–Mo(3)–S	108.5(1)
Mo(2)–Mo(1)–S	54.1(1)	Mo(1)–Mo(3)–S(2)	52.6(1)
Mo(3)–Mo(1)–S	53.9(1)	Mo(2)–Mo(3)–S(2)	98.7(1)
Mo(2)–Mo(1)–S(1)	52.9(1)	S(3)–Mo(3)–S(2)	93.2(1)
Mo(3)–Mo(1)–S(1)	97.7(1)	S–Mo(3)–S(2)	104.8(1)
S–Mo(1)–S(1)	105.2(1)	Mo(2)–S(3)–Mo(3)	72.1(1)
Mo(2)–Mo(1)–S(2)	97.1(1)	Mo(1)–S–Mo(2)	72.2(1)
Mo(3)–Mo(1)–S(2)	53.1(1)	Mo(1)–S–Mo(3)	72.3(1)
S–Mo(1)–S(2)	105.5(1)	Mo(2)–S–Mo(3)	70.0(1)
S(1)–Mo(1)–S(2)	97.2(1)	Mo(1)–S(1)–Mo(2)	73.9(1)
Mo(1)–Mo(2)–Mo(3)	60.9(1)	Mo(1)–S(2)–Mo(3)	74.3(1)
Mo(1)–Mo(2)–S(3)	97.1(1)	Mo(2)–Mo(3)–S(3)	54.0(1)
Mo(3)–Mo(2)–S(3)	54.0(1)	Mo(1)–Mo(3)–S	53.7(1)
Mo(1)–Mo(2)–S	53.7(1)	Mo(2)–Mo(3)–S	55.1(1)
Mo(3)–Mo(2)–S	54.9(1)	S–Mo(2)–S(1)	105.1(1)
S(3)–Mo(2)–S	108.4(1)	Mo(1)–Mo(3)–Mo(2)	60.8(1)
Mo(1)–Mo(2)–S(1)	53.2(1)	O(1)–C–C(1)	118.5(1)
Mo(3)–Mo(2)–S(1)	100.0(1)	O(2)–C–C(1)	116.7(9)
S(3)–Mo(2)–S(1)	94.3(1)		

atoms. All the nonhydrogen atoms except some disordered C atoms of DTP ligand were refined anisotropically. Least-squares refinements were performed by fullmatrix procedures. Crystal structure plots were drawn using ORTEP II [11] software. The positions of all hydrogen atoms were generated geometrically (C–H bond fixed at 0.96 Å), assigned isotropic thermal parameters and allowed to ride on their respective parent C atoms before the final cycle of least-squares refinement. Hydrogen atoms coordinating O were included at idealized positions with an assumed O–H distance of 0.85 Å. Intermolecular S–S distances and dihedral angles were calculated using Molen programs software. The highest peak on the final difference Fourier map in **III** has a height of 1.293 e Å^{-3}, which is located at a position 0.738 Å away from Cl2 (chlorine 2).

RESULTS AND DISCUSSION

Crystal structure

$Mo_3S_4(DTP)_3$(salicylate)(CH_3CN) (**III**). The main structural feature of **III** (shown in Fig. 1) is similar to that of the typical incomplete cubane-type Mo_3S_4 clusters with DTP as the ligand [12]. The bond length of Mo1–N 2.269(7) Å is shorter than the corresponding one in $Mo_3OS_3(DTP)_4(CH_3CN)$, 2.274(6) Å [13]. The substitution of salicylate for bridging DTP decreases its bridged Mo2–Mo3 bond from 2.734(1) Å [14] to 2.693(2) Å, which is almost the same as the average Mo–Mo 2.690 Å when bridged by aliphatic carboxylates [2]. However, the average Mo–μ-S bond 2.292(3) Å of **III** (2.293(2) Å of **IV**, see below) is longer than that of the corresponding ali-

Table 3. Selected bond length (Å) and angles (°) for the complex **IV**

Mo(1)–S(3)	2.290(2)
Mo(1)–S(1)	2.295(2)
Mo(1)–S(4)	2.336(2)
Mo(1)–N(1)	2.358(7)
Mo(1)–Mo(2)	2.7551(10)
Mo(1)–Mo(3)	2.7628(10)
Mo(2)–O(2)	2.215(5)
Mo(2)–S(3)	2.293(2)
Mo(2)–S(2)	2.296(2)
Mo(2)–S(4)	2.345(2)
Mo(2)–Mo(3)	2.6913(9)
Mo(3)–O(1)	2.252(5)
Mo(3)–S(2)	2.292(2)
Mo(3)–S(1)	2.293(2)
Mo(4)–O(5)	2.267(5)
Mo(4)–S(5)	2.294(2)
Mo(4)–Mo(6)	2.6935(11)
Mo(5)–Mo(6)	2.7559(10)
Mo(6)–O(6)	2.235(6)
C8–O3	1.272(10)
C8–O4	1.254(10)
C08–O7	1.253(10)
C08–O8	1.267(11)

S(3)–Mo(1)–S(1)	96.56(8)	C(7)–O(1)–Mo(3)	121.4(5)
S(3)–Mo(1)–S(4)	105.50(7)	C(7)–O(2)–Mo(2)	122.6(5)
S(1)–Mo(1)–S(4)	105.10(7)	C(07)–O(5)–Mo(4)	122.3(5)
S(3)–Mo(1)–Mo(2)	53.10(5)	C(07)–O(6)–Mo(6)	122.8(5)
S(1)–Mo(1)–Mo(2)	96.72(6)	O(2)–C(7)–O(1)	126.8(7)
S(4)–Mo(1)–Mo(2)	54.09(5)	O(2)–C(7)–C(1)	116.1(7)
N(1)–Mo(1)–Mo(2)	93.4(2)	O(1)–C(7)–C(1)	117.0(7)
S(3)–Mo(1)–Mo(3)	97.82(6)	C(1)–C(6)–C(5)	118.9(8)
S(1)–Mo(1)–Mo(3)	52.94(5)	C(1)–C(6)–C(8)	122.5(7)
S(4)–Mo(1)–Mo(3)	53.61(5)	C(5)–C(6)–C(8)	118.4(8)
N(1)–Mo(1)–Mo(3)	134.8(2)	O(4)–C(8)–O(3)	124.5(8)
Mo(2)–Mo(1)–Mo(3)	58.38(2)	O(4)–C(8)–C(6)	119.9(8)
O(2)–Mo(2)–S(3)	172.7(2)	O(3)–C(8)–C(6)	115.6(8)
O(2)–Mo(2)–S(2)	83.5(2)	O(6)–C(07)–O(5)	126.1(8)
S(3)–Mo(2)–S(2)	94.56(8)	O(6)–C(07)–C(01)	116.3(7)
O(2)–Mo(2)–S(4)	82.2(2)	O(5)–C(07)–C(01)	117.6(8)
S(3)–Mo(2)–S(4)	105.13(8)	O(7)–C(08)–O(8)	124.6(9)
S(2)–Mo(2)–S(4)	108.00(7)	O(7)–C(08)–C(06)	118.9(8)
O(2)–Mo(2)–Mo(3)	84.80(14)	O(8)–C(08)–C(06)	116.2(8)
S(3)–Mo(2)–Mo(3)	99.79(6)	S(1)–Mo(3)–S(4)	105.35(8)
S(2)–Mo(2)–Mo(3)	54.01(6)	O(1)–Mo(3)–Mo(2)	84.2(1)
S(4)–Mo(2)–Mo(3)	54.62(5)	S(2)–Mo(3)–Mo(2)	54.15(6)
O(2)–Mo(2)–Mo(1)	134.2(1)	S(1)–Mo(3)–Mo(2)	98.56(6)
S(3)–Mo(2)–Mo(1)	53.00(6)	S(4)–Mo(3)–Mo(2)	55.10(5)
S(2)–Mo(2)–Mo(1)	97.46(6)	O(1)–Mo(3)–Mo(1)	133.3(1)
S(4)–Mo(2)–Mo(1)	53.81(5)	S(2)–Mo(3)–Mo(1)	97.34(6)
Mo(3)–Mo(2)–Mo(1)	60.95(2)	S(1)–Mo(3)–Mo(1)	53.01(6)
O(1)–Mo(3)–S(2)	83.4(2)	S(4)–Mo(3)–Mo(1)	53.80(5)
O(1)–Mo(3)–S(1)	173.0(2)	Mo(2)–Mo(3)–Mo(1)	60.66(2)
S(2)–Mo(3)–S(1)	92.93(8)	S(2)–Mo(3)–S(4)	108.61(7)
O(1)–Mo(3)–S(4)	81.5(2)		

phatic carboxylate-substituted clusters(Mo–μ-S, 2.28 Å) [15, 16, 17], showing the effect on the Mo$_3$S$_4$ core from the bridging ligand and its substituents.

It is structurally unusual [18, 19] that those atoms in **III**, Mo3, Mo2, O1, O2, C, C1, C2, C3, C4, C5, C6 and O3 share a large plane with good coplanarity, as shown by the data listed in Table 4; the dihedral angle between the plane 2 and the plane 3 is 7(2)°. The bond

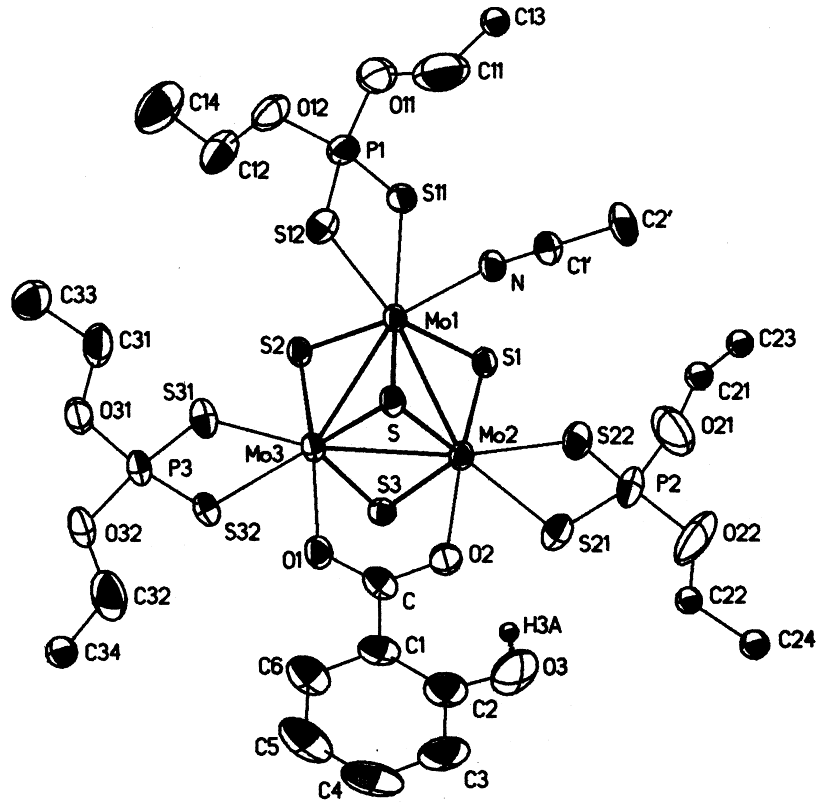

Fig. 1. The ORTEP drawing of compound **III** with a 30% probability level.

Table 4. Dihedral angles calculated for complex **III** and **IV**

Plane No.	Atoms	Plane No.	Dihedral angle (°)
	Complex **III**		
1	Mo1, Mo2, Mo3	2	145.8(1)
2	Mo2, Mo3, O2, O1, C, C1	3	7(2)
3	C, C1, C2, C3, C4, C5, C6	1	139.6(4)
	Complex **IV**		
1	Mo2, Mo3, O1, O2, C1, C7	2	47.6(2)
2	C1, C2, C3, C4, C4, C6, C7, C8	4	92.0(2)
3	Mo4, Mo6, O5, O6, C07, C01	4	46.7(2)
4	C01, C02, C03, C04, C05, C06, C07, C08	5	45.8(2)
5	O3, O4, C8, H3B, O7, O8, C08, H8A	2	46.8(3)

lengths Mo2–O2, Mo3–O1 and bond angles O2–C–C1, O1–C–C1 are different, showing higher asymmetry for plane 2 and 3. These structural details result from the intramolecular H-bond formed between O2 and O3 (distance between O1 and O3 is 2.57 Å). The H-bond, which is coplanar to the phenyl group, forces O3 closer to O1, fixing and tilting the phenyl group to O3 side. As a result, the salicylate ligand has more asymmetry and more coplanarity with Mo2 and Mo3. A dihedral angle of 145.77(14)° between the plane 1 and the plane 2 shows the heavily distorted octahedral coordination of Mo in **III**.

$[Mo_3S_4(DTP)_3(Phthalate)(Py)]_2 \cdot EtOH \cdot CH_2Cl_2$ (**IV**). It is interesting to find that the spare –COOH groups in cluster **IV** still have the capability of forming a dimeric carboxylic acid via H-bonding. The cluster **IV**, as shown in Fig. 2, consists of two incomplete cubane-type $[Mo_3S_4(DTP)_3(phthalate)(Py)]$ units

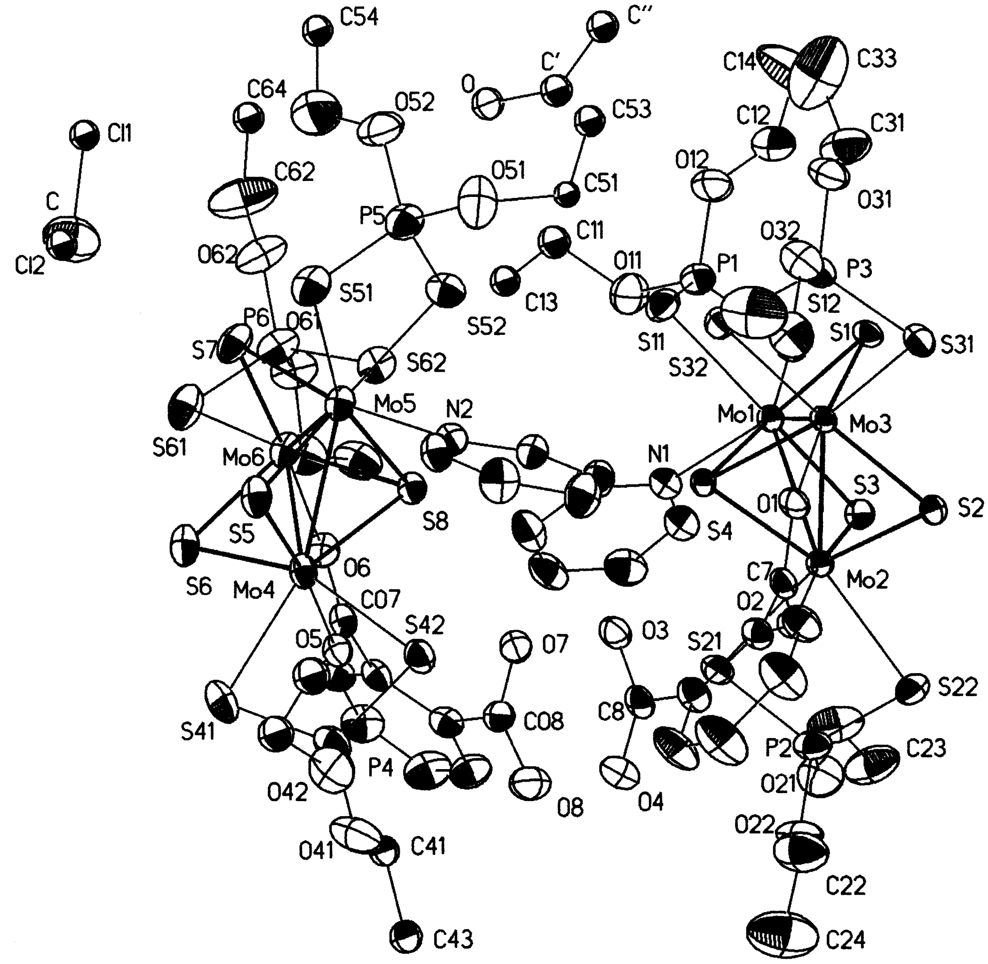

Fig. 2. The ORTEP drawing of compound **IV** with a 30% probability level.

linked together by the intramolecular H-bonds. Two solvent molecules, EtOH and CH_2Cl_2, are situated in the unit cell.

Structural data and dihedrals indicated that two pendant –COOH groups from two phthalate molecules constructed a highly symmetrical rigid plane via intermolecular H-bonding. The structure of this plane was shown in Fig. 3. Although these two H

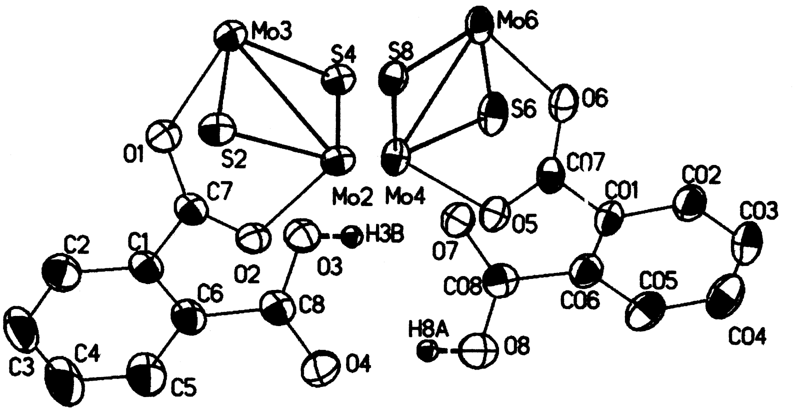

Fig. 3. The ORTEP drawing of two –COOH groups of compound **III** with a 30% probability level.

atoms were theoretically added to the adjacent O atoms (O3–H3B and O4–H8A distances are 0.85 Å, O7–H3B and O4–H8A are 1.84 Å), according to the distance (2.69 Å) of both O3–O7 and O4–O8, we can deduce that the two H atoms H3B and H8A are roughly linear and situated in the same plane with the four O atoms and strong H-bonds are formed. The IR spectra for clusters **III** and **IV** were measured [20] as listed in Table 5. A broad absorption at 3200 cm^{-1} was assigned to v_{OH} for compound **III** and a sharp absorption at 2978 cm^{-1}, which overlaps with the phenyl absorption, was assigned to the v_{OH} for **IV**. This is consistent with the crystal structural results that the H-bond in **IV** is linear and much stronger than that in **III**. The dihedral angles calculated between the two phenyl planes (plane 2 and 4) is 92.0(2)° as shown in Table 4, indicate that the two phenyl planes are aligned perpendicularly in the lattice.

The mean Mo–O bond length 2.242(5) Å (to phthalate ligands) in **IV** is longer than that of the similar aliphatic carboxylate cluster compounds [19] and these four Mo–O bonds, listed in Table 3, differ considerably from each other. This difference is even greater than that of the corresponding Mo–O in cluster **III** as shown in Table 2. This distortion of the coordinated –COO groups is caused by crystalline packing effects. The alignment of the bulky $\mathrm{Mo_3S_4}$ core and the neighboring DTP ligand distort Mo2Mo3O1C7O2 and Mo4Mo6O6CO7O5 planes and also twist the H-bonding plane as shown by the following data: O4O8O3 124.5(8)° ≈ O7OO8O8 124.6(9)°, C8–O3 (1.272(10) Å) ≈ C08–O8 (1.267(11) Å) and C8–O4 (1.254(10) Å) ≈ C08–O7 (1.253(10) Å). As reflected by the dihedral angles between plane 1 and 2, 3 and 4 (Table 4), the $\mathrm{RCO_2}$ group is no longer coplanar as opposed to the case in cluster **III**.

S–S interactions

The intramolecular S–S interactions [21, 22] in $[\mathrm{Mo_3S_4}]$-type (M = Mo, W) clusters are important in crystal packing along with the ligand substitutional effect discussed above. For both **III** and **IV**, S–S interactions, which are all considerably shorter than the corresponding van der Waals contacts [22, 23], were calculated as shown in Fig. 4 and were listed in Table 6. In cluster **III**, the S–S interactions favor the opposite alignment of the two molecules in the cell. On the other side of the molecule, the phenyl ring sterically hinders μ-S atom to form further superamolecular interaction [14], so the two molecules of **III** are packed into the cell with a symmetric center [24]. Similarly, six S–S interactions are found in **IV**. S1, as well as S6, can form two S–S interactions with another two S atoms.

^{31}P NMR

^{31}P NMR spectra of **III** and **IV**, (Fig. 5), were measured in acetone-d$_6$. The assignment of the ^{31}P resonances is consistent with the literature [3]. The resonance (T_1) at 110.08 ppm for **III** was assigned to the two coalesced DTP ligands coordinated to Mo2 and Mo3, respectively; the other resonance (T_2) at 111.33 ppm was assigned to the DTP coordinated to Mo1. Similarly, the resonance (T_1) at 110.82 ppm in **IV** was assigned to the four DTP ligands coordinated to Mo2 and Mo3, Mo4 and Mo6; the other resonance (T_2) at 110.20 ppm was assigned to the DTP ligand coordinated to Mo1, Mo5.

Experimentally, the loosely coordinated ligand L affects the NMR spectrum by its dynamic dissociation in the solution and the carboxylate does so by the long-distance electron delocalization. Normally, the pyridine substitution for acetonitrile will broaden NMR linewidths considerably [3], so significant line-broadening in the spectra of compound **IV** is expected.

For this series of trinuclear clusters, the relative position of T_1 and T_2 is determined by the type of the loosely coordinated ligand L. For compound **III**, L = $\mathrm{CH_3CN}$, T_2 is situated at the lower field to T_1; on the contrary, T_2 is situated at the higher field in the spectra of compound **IV**, L = pyridine. Nevertheless, L can only affect the chemical shift of T_2 considerably, it does little to the chemical shift of T_1, so the chemical shift differences between T_1 and T_2 are mainly attributed to aromatic substituents –OH and –$\mathrm{CO_2H}$. This leads to the conclusion that the $\mathrm{Mo_3S_4}$ core and the superconjugation translate the electron effect to DTP ligands [25]. A more systematic ^{31}P NMR spectroscopic study on more cluster compounds will soon follow.

Acknowledgments—We are grateful for the financial support to the Foundation of the Chinese National Natural Sciences (No. 29303025), the Foundation of Fujian Provincial Natural Sciences (No. 970133) and the Foundation of the Chinese State Key Laboratory of Structural Chemistry (No. 970095).

Table 5. IR vibration of complexes **III** and **IV** (cm^{-1})

		NvMo–(μ_3 – S)	vMo–(μ-S)	vMo–(μ-O)	v(O–H)	v(C–O)	$v\mathrm{C_6H_6}$
III	IR	452	480	641	3200	1169	3000–3030
IV	IR	451	482	642	2978	1159	3000–3050

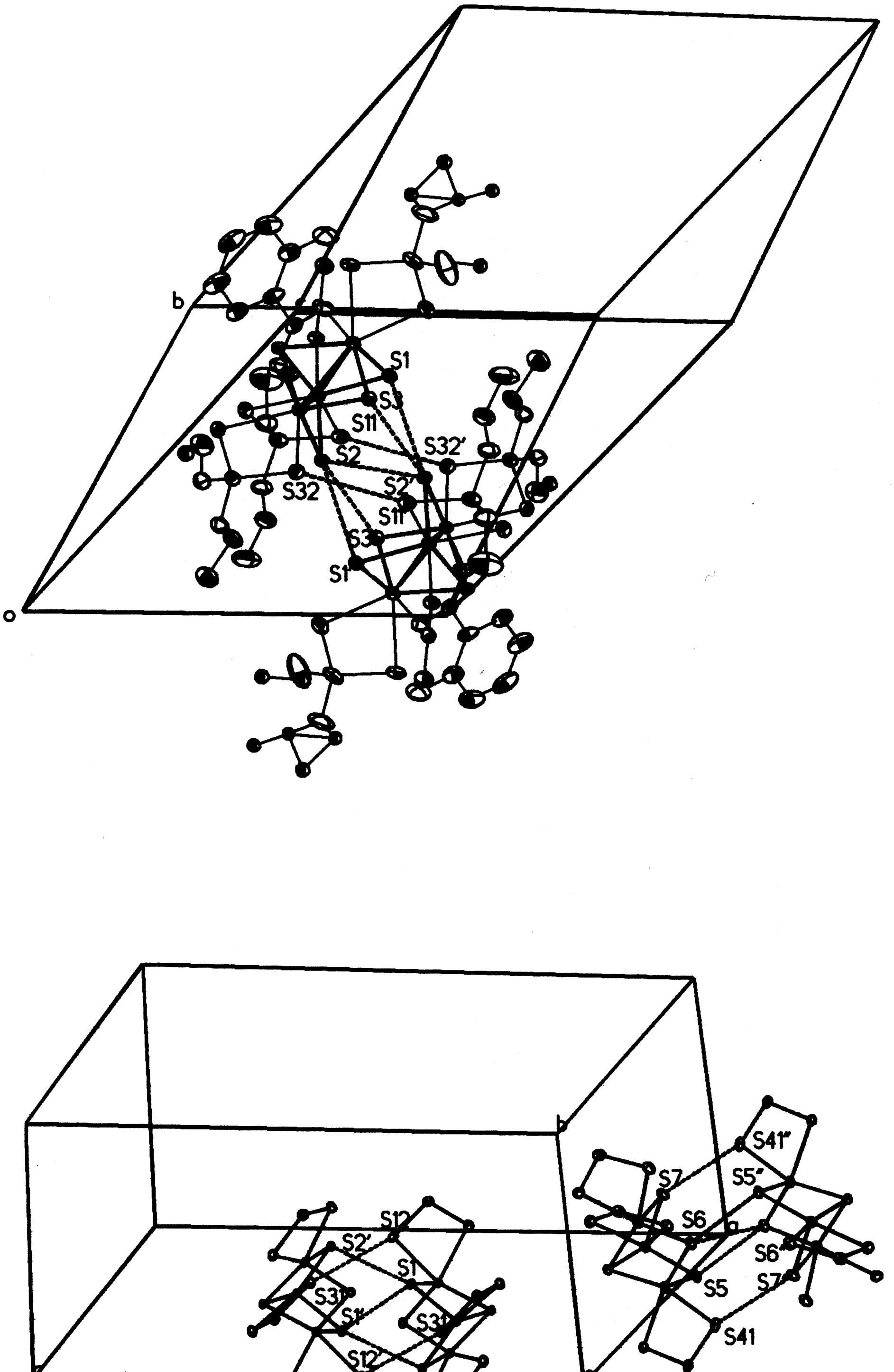

Fig. 4. The ORTEP drawing of S–S interactions in compound **III** and **IV** with a 15% probability level.

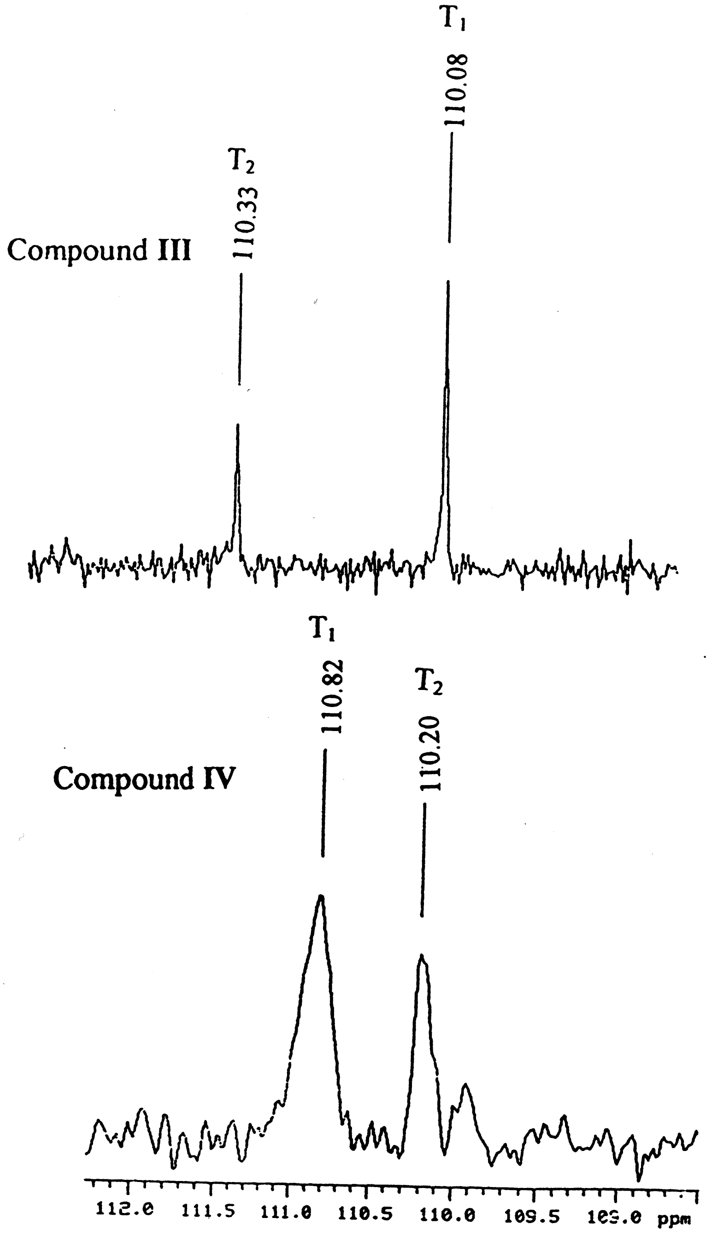

Fig. 5. Decoupled ^{31}P NMR spectra of compound **III** and **IV**.

Table 6. S–S interactions of complex **III** and **IV**

	Complex **III**		Complex **IV**	
Symmetry operations	S atoms	distance (Å)	S atoms	distance (Å)
$(1-x, 1-y, 1-z)$	S1–S2′	3.646(2)	S1–S1′	3.229(3)
S2–S2′	3.264(3)	S1–S2′	3.416(3)	
S2–S3′	3.364(2)	S12–S13′	3.611(4)	
S11–S32′	3.529(7)			
$(2-x, -y, -z)$			S5–S6″	3.450(4)
		S6–S6″	3.419(4)	
			S7–S41″	3.667(4)

The authors also wish to express their appreciation to Professor M. C. Hong, Dr J. T. Chen and Mr Q. M. Wang for the data collection and structure analysis.

REFERENCES

1. Keck, H., Kuchen, W., Mathow, J. and Wunderlich, H., *Angew. Chem. Int. Ed. Engl.*, 1982, **12,** 929.
2. Huang, J.-Q., Huang, J.-L., Shang, M.-Y., Lu, S.-F., Lin, X.-T., Lin, Y.-H., Huang, M.-D., Zhuang, H.-H. and Lu, J.-X., *Pure Appl. Chem.*, 1988, **60,** 1185–1192.
3. Yao, Y.-G., Akashi, H., Sakane, G., Shibahara, T. and Ohtaki, H., *Inorg. Chem.*, 1995, **34,** 42–48.
4. Murata, T., Gao, H., Mizobe, Y., Nakano, F., Motomura, S., Tanase, T. and Yano, S., Hidai, M., *J. Am. Chem. Soc.*, 1992, **114,** 8287–8288.
5. Murata, T., Mizobe, Y., Gao, H., Ishii, Y., Wakabayashi, T., Nakano, F., Tanase, T., Yano, S., Hidal, M., Echizen, I., Nanikawa, H. and Motomura, S., *J. Am. Chem. Soc.*, 1992, **116,** 3389–3398.
6. Shi, S. and Ji, W., Tang, H., *J. Am. Chem. Soc.*, 1994, **116,** 3615–3616.
7. Bacon, W. E. and Lesure, W. M., *J. Am. Chem. Soc.*, 1954, **76,** 670–676.
8. Sheldrick, G. M., *SHEXLXTL/PC. Users Manual*, Siemens Analytical X-ray Instruments, Madison, WI, 1990.
9. Sheldrick, G. M., in *Computational Computing* 3. *Data Collection*, *Structure Determination*, *Proteins and Databases*, ed. G. M. Sheldrick, C. Kreuger and R. Goddard. Oxford University Press, New York, 1985, pp. 175–189.
10. Sheldrick, G. M., *SHELXLT-Plus. PC Version*, Siemens Analytical X-ray Instruments, Madison, WI, 1987.
11. Johnson, C. K., *ORTEP II. Report ORNI*-5138. Oak Ridge National Laboratory, 1976.
12. Shibahara, T., *Adv. Inorg. Chem.*, 1991, **37,** 143–173.
13. Shibahara, T., private communication.
14. Lin, X.-T., Lin, Y.-H., Huang, J.-Q. and Huang, J.-Q., *Kexue Tongbao*, 1986, **7,** 509.
15. Lu, S.-F., Shang, M.-Y., Huang, J.-Q., Huang, J.-L. and Lu, J.-X., *Sci. Sin. B*, 1988, **XXXI,** 147.
16. Birnbanum, A., Cotton, F. A., Dori, Z., Kapon, M., Marler, D., Reisner, G. M. and Schwotzer, W., *J. Am. Chem. Soc.*, 1985, **107,** 2405.
17. Wu, D.-M., Zhuang, H.-H., Zheng, J.-J., Huang, J.-L., Lu, J.-X. and Huang, J.-Q., *Sci. Sin. B*, 1985, **7,** 589.
18. Lu, S.-F., Huang, J.-Q., Huang, X.-Y. and Wu, Q.-J., *JieGou HuaXue* (*Chin. J. Struct. Chem.*), 1995, **14,** 482–487.
19. Lu, S.-F., Huang, J.-Q., Huang, M.-D. and Huang, J.-L., *Acta Chim. Sin. Engl. Ed.*, 1989, **1,** 24.
20. Huang, J.-L., Huang, J.-Q., Shang, M.-Y. and Lu, J.-X., *Adv. Sci. China Chem.*, 1990, **3,** 155–180.
21. Fedin, V. P., Sokolov, M. N. and Virovets, A. V., *Inorg. Chim. Acta.*, 1992, **194,** 195.
22. Cotton, F. A. and Wilkinson G., *Advanced Inorganic Chemistry*, John Wiley and Sons, 1962, p. 104.
23. Casas, J. S., Castineirtas, A., Haiduc, I., Sonchez, A. and Sordo, J., *Polyhedron*, 1994, **13,** 1805–1809.
24. Lu, S.-F., Wu, Q.-J., Chen, H.-B., Yu, R.-M. and Huang, J.-Q., *JieGou HuaXue* (*Chin. J. Struct. Chem.*), 1994, **13,** 389–396.
25. Lu, J.-X., *JieGou HuaXue* (*Chin. J. Struct. Chem.*), 1989, **8,** 327–339.